Extended abstract submitted for the proceedings of the Ocean Optics XXII conference held in Portland, USA, 26-31 October 2014

First optical observations in the turbidity maximum zone in the Río de la Plata estuary: A challenge for atmospheric correction algorithms

A. I. Dogliotti[1*], M. Camiolo[2], C. Simionato[3], A. Jaureguizar[2,4], R. Guerrero[2], C. Lasta[2]

[1] Instituto de Astronomía y Física del Espacio (IAFE), CONICET/UBA, Argentina
[2]Instituto Nacional de Investigación y Desarrollo Pesquero (INIDEP), Argentina
[3] Centro de Investigaciones del Mar y la Atmósfera (CIMA/CONICET-UBA), Argentina
[4]Comisión de Investigaciones Científicas (CIC), Argentina

[*]Corresponding author e-mail: adogliotti@iafe.uba.ar

ABSTRACT

The Río de la Plata (RdP) estuary, located at 35°S on the southwestern Atlantic Ocean, is a shallow and large-scale plain, which drains the second largest basin in South America. The RdP river carries high amounts of nutrients, suspended particulate and dissolved organic matter to the adjacent shelf waters and is considered among the most turbid estuaries in the world. A turbidity maximum and a sharp surface front defining its seaward edge is a distinctive feature of this estuary. Such high sediment loads represent a challenge to atmospheric correction algorithms which usually rely on the assumption of zero water-leaving reflectance in the near infrared (NIR) or short wave infrared (SWIR) parts of the spectrum. Uncertainties of the primary remote sensing products have never been quantified in RdP before due to lack of *in situ* measurements. In February and April 2013 two field campaigns were performed in the turbidity maximum zone where water reflectance was measured and surface water samples were collected for turbidity and total suspended particle concentration determinations. A match-up analysis was performed to evaluate the performance of five atmospheric correction algorithms on MODIS-Aqua data that use the NIR and/or SWIR bands to estimate the aerosols optical properties in a pixel-by-pixel basis and from clear water pixels and then applied to the whole image. Satellite retrievals of remote sensing reflectance at the visible bands of Aqua sensor generally showed quite large uncertainties and constant underestimation (largest at the blue bands), whereas the uncertainties in the NIR bands were the lowest.

INTRODUCTION

Validation of primary ocean color products is very important to retrieve reliable satellite derived optical properties and concentration of optically significant constituents. From the total reflectance sensed by an ocean color remote sensor, over 80% of the signal comes from the contribution of scattering by air molecules and aerosols, while the useful signal (water reflectance) is only a small part of it. Traditional atmospheric correction (AC) algorithms rely in the assumption of zero reflectance at the near infrared (NIR) wavelengths (black pixel) or modeling it (bright pixel). These AC algorithms usually fail in coastal turbid waters due to the presence of highly scattering sediments which cause high water reflectance in NIR wavelengths leading to an over-estimation of the aerosol reflectance and thus in retrieving low and even negative water reflectance values in the short wavelengths (λ < 500 nm). In order to overcome this difficulty in turbid waters, it was proposed to replace the assumption of zero water reflectance at the NIR wavelengths by the assumption of zero water reflectance at the short wave infrared (SWIR) wavelengths where water absorption is higher (Wang 2007).

The Río de la Plata (RdP) estuary, located at 35°S on the eastern coast of South America, carries high amounts of nutrients, suspended particulates and dissolved organic matter to the adjacent shelf waters. The amount of sediments transported by the RdP has been estimated to range between 80 and 160 million tons y^{-1}, which makes this estuary one of the most turbid in the world with mean concentrations of total suspended matter (TSM) ranging from 100 to 300 mg L^{-1} and up to 400 mg L^{-1} (Framiñan and Brown 1996). The highly turbid waters of RdP represent a challenge and an ideal scenario to test atmospheric correction algorithm performance (Shi and Wang 2009, Moore *et al*. 2010, Doron *et al*. 2011, Jiang and Wang, 2014).

In a qualitative analysis, Dogliotti *et al.* (2011) showed that in the RdP plume waters the standard NIR atmospheric correction (Bailey *et al.* 2010) completely failed in retrieving water reflectance mainly due to sensor saturation and an incorrect estimation of the marine contribution in the NIR. In turn, the standard SWIR approach (Wang 2007) showed better results, but unphysical correlations between marine features and atmospheric products, such as aerosol reflectance, in the most turbid part of the estuary were clearly identified. The use of an iterative SWIR-based atmospheric correction approach that accounts for non-zero water reflectance in the SWIR bands was proposed and seemed to be a good alternative for retrieving accurate marine reflectance, although the lack of field data prevented a quantitative analysis (Dogliotti *et al.* 2011). In the present work the validation of different atmospheric correction algorithms is performed for the first time using *in situ* water reflectance measurements in the highly turbid waters of RdP.

In the following sections, a short description of the five atmospheric correction algorithms analyzed is presented followed by details on the *in situ* measurements used to evaluate the algorithms and the match-up protocol. In the last two sections results of the comparison and a discussion on the limitations are presented.

ATMOSPHERIC CORRECTION ALGORITHMS

The sampling site was located in highly turbid waters as indicated field and satellite data (T_{ind}>1.3), thus five different atmospheric correction approaches based on estimations of aerosol properties in the NIR and/or SWIR and subsequently extrapolating these properties from the SWIR to shorter wavelengths were evaluated. The different approaches varied according to whether the aerosol optical properties are estimated from the NIR or the SWIR part of the spectra and whether the aerosol type is allowed to vary in space (denoted as V) or fixed (denoted as F), and also whether both the aerosol type and concentration are fixed in space (denoted FF). Thus, the following five algorithms have been applied and evaluated in the present study:

1) SWIR-V: the aerosol type, determined by the Ångström coefficient at 531, $\alpha(531)$, is retrieved in a pixel-by-pixel basis and calculated using the 1240 and 2130 nm bands.

For the following four algorithms, the aerosol properties are estimated from a region of clear water pixels (30x20 pixels) which are located in the center of Samborombón Bay (white rectangle in Figure 1). In these cases, the atmospheric correction is run twice. The first one is applied to the clear water pixels to obtain the aerosol optical properties using either the SWIR or NIR bands and then a second run is performed to calculate R_{rs} for all the pixels using either the $\alpha(531)$ and the 2130 nm band, or the aerosol optical thickness (τ_a) at every band obtained from the clear water pixels. The different approaches for the aerosol determination in the clear waters are specified as:

2) SWIR-F: it uses a fixed $\alpha(531)$ calculated using SWIR bands 1240 and 2130 nm (Wang 2007) assuming zero water reflectance in these bands.

3) SWIR-FF: it uses fixed τ_a at each band calculated using SWIR bands 1240 and 2130 nm (Wang 2007) assuming zero water reflectance in these bands.

4) NIR-F: it uses a fixed $\alpha(531)$ calculated using the NASA standard AC, i.e. NIR bands (Bailey *et al.* 2010)

5) NIR-FF: it uses a fixed τ_a at each band calculated using the NASA standard AC, i.e. NIR bands (Bailey *et al.* 2010)

DATA

In situ data were collected during two cruises in the turbidity maximum zone of the RdP. Locations of the stations and measurements performed can be found in Figure 1 and Table 1. Water reflectance (350-2500 nm) was measured with an ASD Fieldspec FR spectrometer. The downwelling irradiance above the surface (E_d) was measured using a Spectralon reference panel. Then, the total upwelling radiance from the water ($L_u(\lambda)$) (*i.e.* from the water and from the air–sea interface) was measured by pointing the sensor at the water surface at 40° from nadir, maintaining an azimuth of 90° from the solar plane with respect to the sun. Downwelling sky radiance ($L_{sky}(\lambda)$) was measured at a zenith angle of 40° to account for the skylight reflection. The reflectance (ρ_w) was calculated using the following equation (Mobley, 1999):

$$\rho_w(\lambda) = \frac{L_u - (\rho_{sky} L_{sky})}{E_d} \quad [1]$$

where ρ_{as} is the air–sea interface reflection coefficient that was set to a fixed value of 0.0256 (no data on wind speed was available). An extra correction was performed for residual sky glint by subtracting the reflectance remaining at 1305 nm, supposing that sky glint is relatively white in spectral shape under cloudy conditions (Toole *et al.*, 2000). Quality control of the data included only marine reflectance that were collected in homogeneous sunny skies (as indicated by the relation L_{sky}/E_d (750)< 0.05 sr^{-1}), and with small deviation from the time-averaged mean reflectance at 780 nm and in the visible and near infrared range (400-900 nm), *i.e.* a coefficient of variation (standard deviation to mean ratio) CV < 10% and 50%, respectively. The hyperspectral reflectance data were integrated over the relative spectral response function of MODIS bands.

Water samples were collected just beneath the water surface in coincidence with the water reflectance measurements. Right after the cruise, turbidity was measured from the water samples and were also filtered, stored and transported to the laboratory at the National Fisheries Research Institute (INIDEP) for total suspended matter (TSM) analysis. TSM concentration (mg L^{-1}) was determined gravimetrically using pre-ashed APFF02500 Millipore glass fiber filters (nominal pore size of 0.7µm) following the protocol described in Tilstone *et al.* (2003) based on van der Linde *et al.* (1998). Turbidity (T) was measured with a portable HACH 2100P ISO turbidimeter. Three replicate measurements were recorded for each sample.

MODIS-Aqua spatially extracted Level-1A files were acquired for RdP estuary (Figure 1) from the NASA ocean color web page (oceancolor.gsfc.nasa.gov) for the dates with concurrent *in situ* turbidity measurements (Table 1). The SeaDAS 7.01 software was used to generate Level-2 files containing spectral Rayleigh-corrected (ρ_{rc}) reflectance, the turbidity index (T_{ind}), remote sensing reflectance (R_{rs}), Ångström coefficient at 531 ($\alpha(531)$), and aerosol optical

thickness (τ_a) at all bands. Water reflectance (ρ_w) was calculated from the remote sensing reflectance (R_{rs}) as $\rho_w = R_{rs}\,\pi$. The STRAYLIGHT and HILT flags were not used as masks given that the highly reflective (turbid) waters and sensor saturation erroneously mask most of the RdP estuary. The cloud-masking was performed using the Rayleigh-corrected reflectance (dimensionless) at 2130 nm and a threshold of 0.018 given that the operational scheme usually masks the highly turbid waters as clouds.

For the match-up analysis, the median value of each product in a 3×3 pixel box centered at the location of the sample sites and with ±3 h time difference between the satellite overpass and the sampling was extracted and used to compare with field measurements. Quality of the satellite retrieval was assessed using the flags for land (LAND), sun glint (HIGLINT), high sensor view zenith angle (60°) (HISATZEN), and high solar zenith (70°) (HISOLZEN), a minimum number of pixels (5 out of 9) should be valid and the standard deviation should be below 20% of the mean to consider it a valid match-up.

RESULTS

The spectral signatures (Figure 2) show typical features characteristic of highly turbid waters, *e.g.* Doxaran *et al*. (2002). In general, R_{rs} increases with turbidity and the wavelength of the main peak increases from green to red and NIR wavelengths with increasing T. The reflectance increases between 400 and 700 nm for samples with T varying from 26 to 250 FNU and then the reflectance tends to saturate and then increases again between 750 and 950 nm. A second and a third peak in R_{rs} can be observed at 800 nm and 1071 nm, which are characteristic of highly turbid waters, the former traditionally observed and the latter recently described in Knaeps *et al.* (2012). As can be clearly observed, reflectance is far from zero in the NIR and the SWIR regions (950–1200 nm) and it depends on turbidity.

Satellite retrievals of remote sensing reflectance from the MODIS-Aqua sensor using the five AC showed a constant underestimation in all bands, being largest at the blue and decreasing towards the NIR bands (Figure 3). The SWIR-V approach showed the highest negative mean relative percentage error (MRE%) in the blue-green bands and the NIR-F in the red-NIR bands. The approaches using a spatially fixed aerosol model and optical thickness (FF) showed better results, being lowest at 859 nm band (-7.5% and -6.3% for SWIR-FF and NIR-FF, respectively). In general, slightly better results were found for SWIR-FF in the blue-green bands and for the NIR-FF in the red-NIR bands (Figure 3). Figure 4 further shows the match-up comparison for seven bands and for the different AC approaches analyzed. Negative retrieved R_{rs} values in the blue bands (412 and 443 nm) were found when applying SWIR-V probably due to non-zero contribution of R_{rs}(1240) and slightly negative value sin the blue using NIR-F.

Two examples of the match-up comparison between retrieved R_{rs} spectra and *in situ* data are shown in Figure 5. Field measurements along the transect between station 11 (closet to land) and 7 (more offshore) show a general decrease in turbidity from land to offshore with a peak at station 9 for which high R_{rs}(859) values can also be observed. The R_{rs} was under-estimated by all AC algorithms at all bands in station 9, which showed the highest turbidity (602 FNU), while at station 7, with the lowest turbidity of the whole cruise (16 FNU), R_{rs} values were also under-estimated in the VIS bands but a good agreement was found for the NIR bands, specially for the NIR-FF and SWIR-FF algorithms.

DISCUSSION

The poor performance of SWIR-V approach can be related to non-zero reflectance in the 1240 nm band in highly turbid waters as has been previously found (Shi and Wang 2009, Dogliotti *et al.* 2011) and is confirmed in this study (Figure 6). Rayleigh-corrected band at 1240 nm shows high values that are correlated with high marine reflectance at the turbidity maximum and other features which are clearly observed at 869 nm, but not detected at 2130 nm. The spectral slope of the aerosol scattering determined using the bands at 1240 and 2130 nm becomes large due to reflectance at 1240 nm which results in an over-estimated aerosol reflectance at the VIS/NIR bands when extrapolating from R_{rs}(2130) and thus in an under-estimated water reflectance in general, which may lead to negative values in the blue bands.

The general under-estimation of retrieved R_{rs} for all the AC analyzed is possibly due to the following: 1) failure of assumptions made for the retrieval of aerosol properties in the "clear pixels", like negligible water reflectance in the SWIR bands and the modeled non-zero reflectance in the NIR; 2) difference between the aerosol type over the match-up pixels and the one determined from the clear pixels (non-spatial homogeneity of the aerosol type and concentration); 3) problems in the extrapolation of aerosol reflectance from the SWIR to the VIS/NIR given the large wavelength difference. The error in the aerosol model selected and thus in the estimated aerosol reflectance increases with decreasing wavelength due to the extrapolation procedure. Lower accuracy in the short wavelengths compared to the long wavelengths could also be due to degradation of the blue bands (Meister, 2011). The slightly better results observed using fixed aerosol model and concentration compared to just fixing the aerosol model and deserves further analysis.

CONCLUSIONS

In the present study the first optical observations in the turbidity maximum zone in the Río de la Plata estuary have been presented and five ocean color atmospheric correction algorithms applied to MODSI-Aqua have been evaluated. Measured surface TSM concentrations were higher than those previously reported in the literature (940 mg L^{-1}) and reflectance spectra showed typical characteristics of highly turbid waters with high non-zero values in the NIR.

The validation of different NIR/SWIR extrapolative approaches for the atmospheric correction scheme showed a constant underestimation of the measured R_{rs} values. The largest errors were found in the visible bands (largest in the blue), while lower errors were found in NIR bands. The standard SWIR-V approach (which calculates the aerosol model in a pixel-by-pixel basis) showed the worst performance probable due to non-zero water reflectance in the 1240 nm band. In turn, extrapolation of aerosol properties (type and/or concentration) from clear water pixels showed better results. A better performance was found using a fixed type and aerosol concentrations estimated using either the SWIR or NIR bands in near clear waters with relative percentage errors ~ -20% in the VIS and ~ -10% in the NIR, and with the lowest error in the 859 nm band (~-7%). Assumptions made in the clear pixels and how representative (spatially) they are should be carefully analyzed in future works.

ACKNOWLEDGEMENTS

This study was supported by the ANPCyT (National Agency for Scientific and Technological Research of Argentina) PICT 2010-1831. NASA is acknowledged for the MODIS-Aqua satellite data.

REFERENCES

Bailey, S.W., Franz, B.A. and Werdell, P.J. (2010). Estimation of near-infrared water-leaving reflectance for satellite ocean color data processing. Optics Express, 18, 7521-7527.

Dogliotti, A. I., Ruddick, K., Nechad, B., and Lasta, C. (2011). Improving water reflectance retrieval from MODIS imagery in the highly turbid waters of La Plata River. Proceedings of VI International Conference "Current Problems in Optics of Natural Waters". St. Petersburg, Russia: Publishing House "Nauka" of RAS.

Doron, M, S. Bélanger, D. Doxaran and M. Babin (2011). Spectral variations in the near-infrared ocean reflectance. Remote Sensing of Environment, 115(7):1617-631.

Doxaran, D., Froidefond, J. M., Lavender, S., Castaing, P. (2002). Spectral Signature of Highly Turbid Waters Application with SPOT Data to Quantify Suspend Particulate Matter Concentrations. Remote Sensing of Environment, 81: 149-161

Framiñan, M., and O. Brown (1996), Study of the Río de la Plata turbidity front, Part 1: Spatial and temporal distribution, *Cont. Shelf Res.*, 16, 1259– 1282, doi:10.1016/0278-4343(95)00071-2.

Jiang, L. and Wang, M. (2014). Improved near-infrared ocean reflectance correction algorithm for satellite ocean color data processing. *Optics Express*, Vol. 22, 18, 21657-21678.

Knaeps, E., Raymaekers, D., Sterckx, S., Ruddick, K., Dogliotti, A. I. (2012). In-situ evidence of non-zero reflectance in the OLCI 1020 nm band for a turbid estuary. Remote sensing of Environment, Sentinel Special issue, 120: 133-144.

Meister, G. (2011). Calibration and characterization adjustments to the MODIS ocean color bands by the OBPG. In *Proc. MODIS Sci. Team Meet.*, 1-23.

Mobley, C.D. (1999). Estimation of the remote-sensing reflectance from above- surface measurements, *Appied Optics*, 38, 7442-7455.

Moore, G., S. Lavender, S. Kratzer, J. Icely, J-P. Huot. (2010). The MERIS bright pixel atmospheric correction: evolution, performance assessment and validation for the MERIS 3rd reprocessing. Proceedings of the Ocean Optics XX conference held in Anchorage, USA, 27th September - 1st October 2010.

Shi, W., Wang, M. (2009). An assessment of the black ocean pixel assumption for MODIS SWIR bands. Remote Sensing of Environment, 113: 1587–1597

Tilstone, G., Moore, G., Sorensen, K., Doerffer, R., Rottgers, R., Ruddick, K. G., et al. (2003). REVAMP Regional Validation of MERIS Chlorophyll products in North Sea coastal waters: Protocols document. Paper presented at the MERIS and AATSR Calibration and Geophysical Validation (MAVT-2003), Frascati.

Toole, D. A., Siegel, D. A., Menzies, D. W., Neumann, M. J., and Smith, R. C. (2000). Remote sensing reflectance determinations in the coastal ocean environment: Impact of instrumental characteristics and environmental variability. Applied Optics, 3(39), 456–469.

Van der Linde, D. W. (1998). Protocol for the determination of total suspended matter in oceans and coastal zones (Technical Note No. I.98.182): Joint Research Centre, Ispra.

Wang, M. (2007). Remote sensing of the ocean contributions from ultraviolet to near infrared using the shortwave infrared bands: simulations. Applied Optics, 46, 1535–1547.

Table 1. Summary of the cruises conducted in maximum turbidity zone indicating the cruises date, measured turbidity (T) and total suspended matter (TSM) range (minimum-maximum), and number of sampled stations.

Date	*T [FNU]*	*TSM[mg L^{-1}]*	*# St.*
27 Feb 2013	16-602	16-664	11
30 Apr 2013	41- >1000	25-940	12

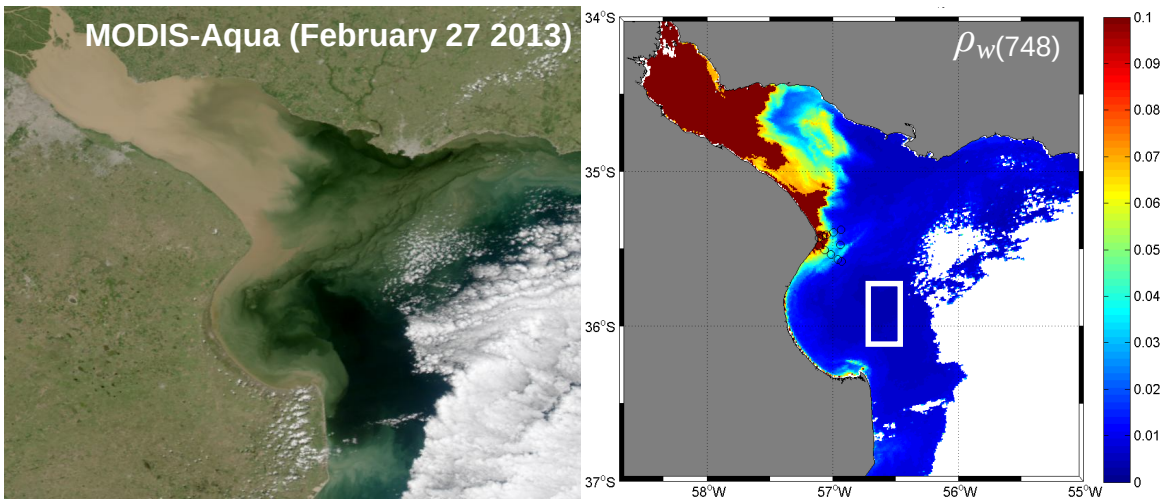

Figure 1. a) True color image of MODIS data on February 27, 2013. b) Rayleigh-corrected reflectance at 748 nm image of the data in a. Location of sampled stations are shown (circles) as well as the region where the "clear pixels" were selected for the AC algorithms (white rectangle). Band saturation is shown in brown in b).

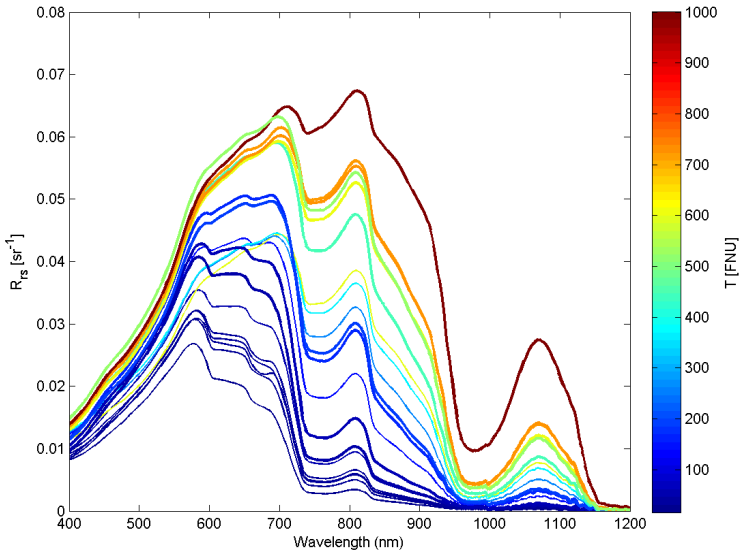

Figure 2. Above-water reflectance spectra $R_{rs}(\lambda)$ corresponding to different turbidity values collected in February 27, 2013 (thin lines) and April 30, 2013 (bold lines)

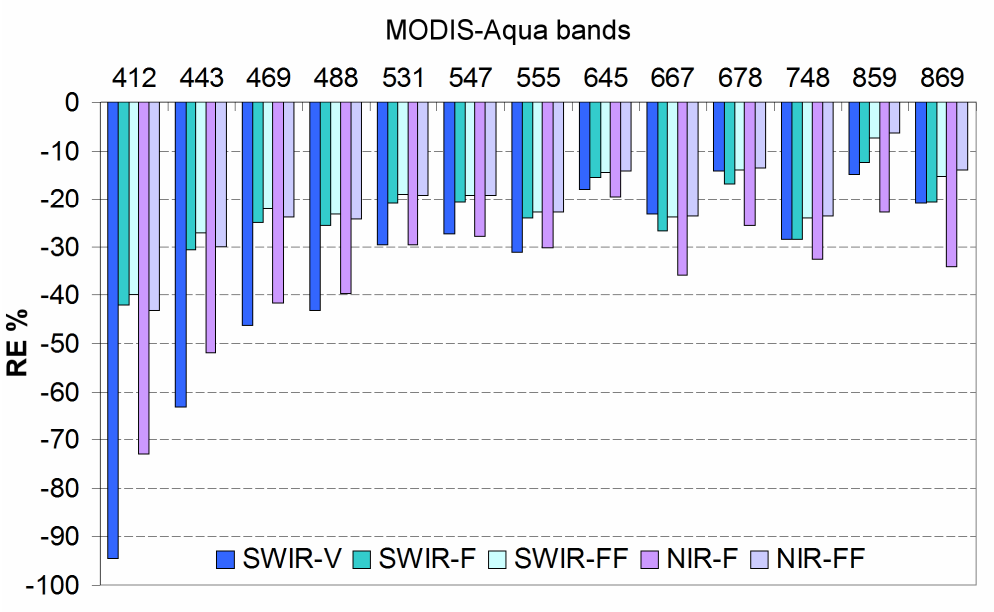

Figure 3. Mean relative percentage error (RE) for the VIS/NIR bands and for different atmospheric correction algorithms (see text for details).

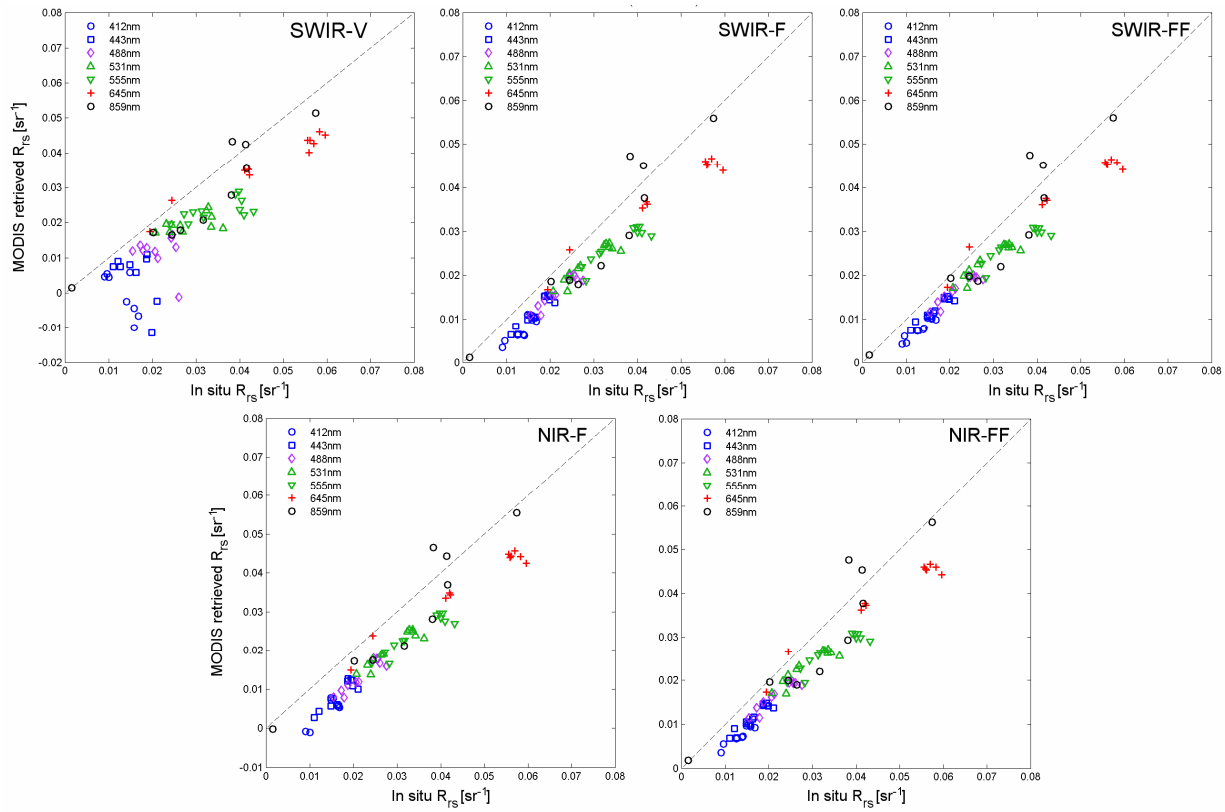

Figure 4. Scatter plots of MODIS-Aqua derived using the different algorithms analyzed against *in situ* R_{rs} at 412, 443, 488, 531, 555, 645 and 859 nm.

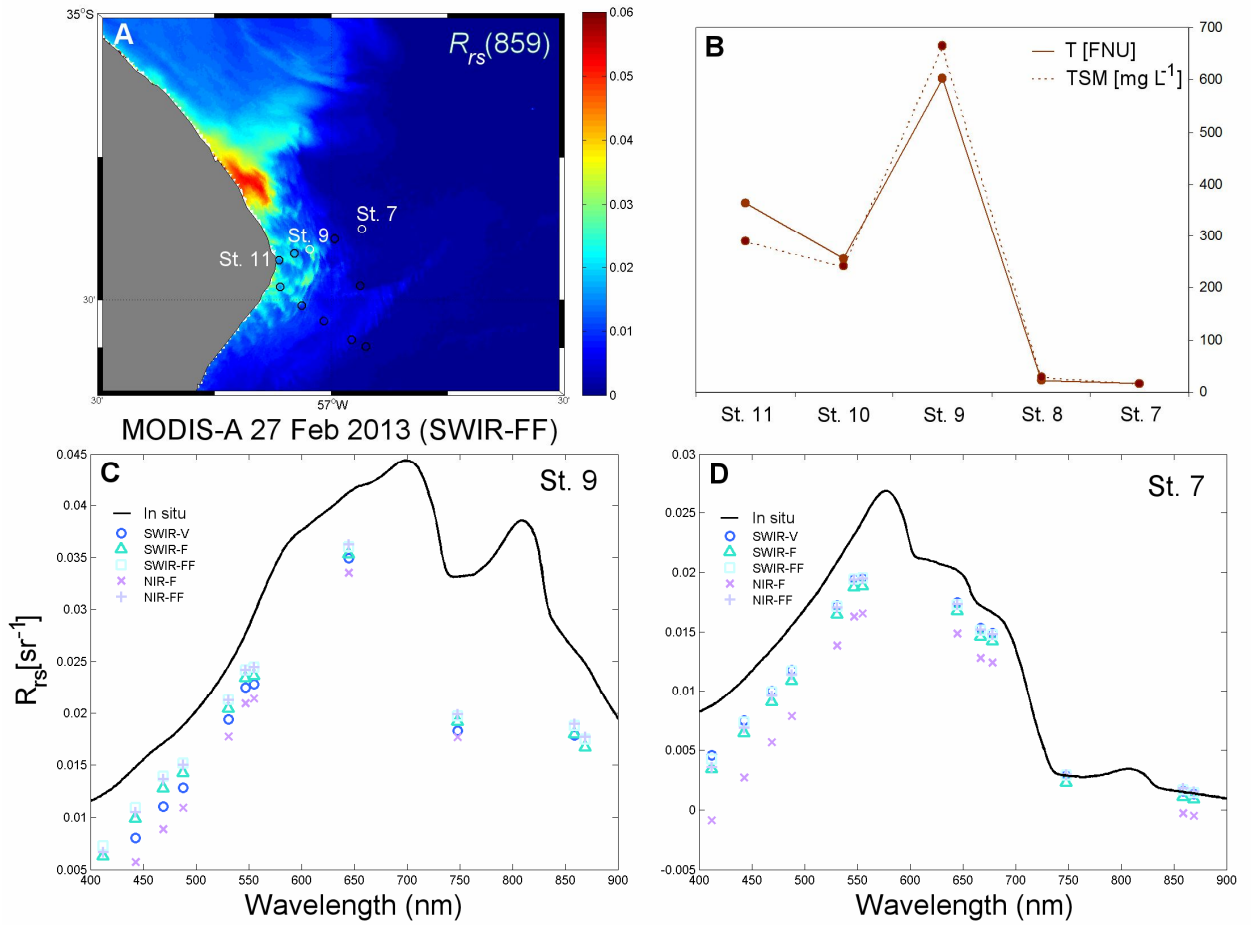

Figure 5. A) MODIS-Aqua derived R_{rs} at 859 nm image using the SWIR-FF atmospheric correction algorithm acquired on February 27, 2013 with stations number and locations indicated (black circles). B) Measured turbidity and total suspended matter at stations 7-11. Comparisons between MODIS-retrieved R_{rs} spectra using different AC and *in situ* data for stations C) 9 and D) 7.

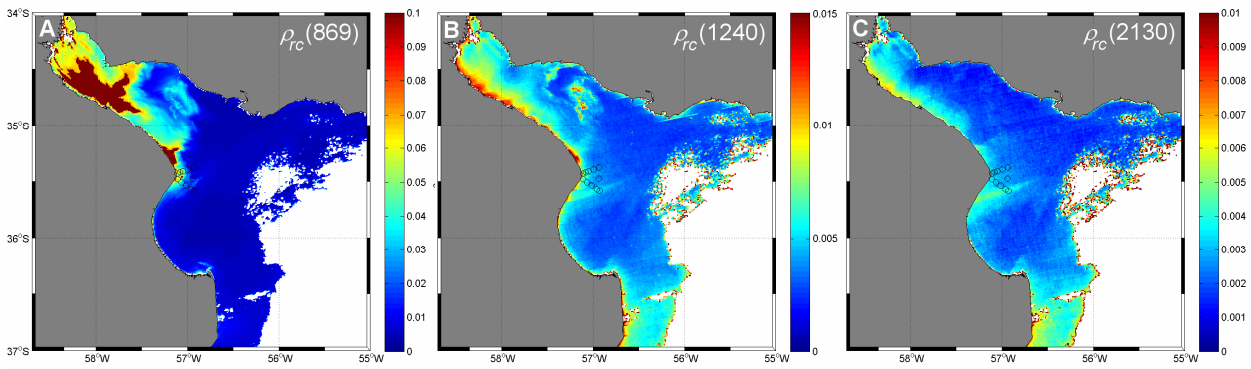

Figure 6. MODIS-Aqua derived Rayleigh-corrected reflectance image acquired on February 27, 2013 at A) 869 nm, B) 1240 nm, and C) 2130 nm.